INFECTION AND IMMUNITY, Sept. 1997, p. 3561–3570 Vol. 65, No. 9
0019-9567/97/$04.00+0

Bacteroides fragilis Toxin Exhibits Polar Activity on Monolayers of Human Intestinal Epithelial Cells (T84 Cells) In Vitro

FRANCES G. CHAMBERS,[1,2] SHERIN S. KOSHY,[2] ROXAN F. SAIDI,[2] DOUGLAS P. CLARK,[3] RICHARD D. MOORE,[4] AND CYNTHIA L. SEARS[1,2]*

Divisions of Infectious Diseases,[1] Gastroenterology,[2] and Internal Medicine,[4] Department of Medicine, and Divisions of Medical Microbiology and Cytopathology,[3] Department of Pathology, The Johns Hopkins University School of Medicine, Baltimore, Maryland 21205-2196

Received 18 February 1997/Returned for modification 14 April 1997/Accepted 19 June 1997

Strains of *Bacteroides fragilis* associated with diarrhea in children (termed enterotoxigenic *B. fragilis*, or ETBF) produce a heat-labile ca. 20-kDa protein toxin (BFT). The purpose of this study was to examine the activity of BFT on polarized monolayers of human intestinal epithelial cells (T84 cells). In Ussing chambers, BFT had two effects. First, BFT applied to either the apical or basolateral surfaces of T84 monolayers diminished monolayer resistance. However, the time course, magnitude, and concentration dependency differed when BFT was applied to the apical versus basolateral membranes. Second, only basolateral BFT stimulated a concentration-dependent and short-lived increase in short circuit current (I_{sc}; indicative of Cl^- secretion). Time course experiments indicated that I_{sc} returned to baseline as resistance continued to decrease, indicating that these two electrophysiologic responses to BFT are distinct. Light microscopic studies of BFT-treated monolayers revealed only localized cellular changes after apical BFT, whereas basolateral BFT rapidly altered the morphology of nearly every cell in the monolayer. Transmission and scanning electron microscopy after basolateral BFT confirmed a striking loss of cellular microvilli and complete dissolution of some tight junctions (zonula occludens) and zonula adherens without loss of desmosomes. The F-actin structure of BFT-treated monolayers (stained with rhodamine-phalloidin) revealed diminished and flocculated staining at the apical tight junctional ring and thickening of F-actin microfilaments in focal contacts at the basolateral monolayer surface compared to those in similarly stained control monolayers. BFT did not injure T84 monolayers, as assessed by lactic dehydrogenase release and protein synthesis assays. These studies indicate that BFT is a nonlethal toxin which acts in a polar manner on T84 monolayers to stimulate Cl^- secretion and to diminish monolayer resistance by altering the apical F-actin structure of these cells. BFT may contribute to diarrheal disease associated with ETBF infection by altering epithelial barrier function and stimulating Cl^- secretion.

Strains of *Bacteroides fragilis* (termed enterotoxigenic *B. fragilis*, or ETBF) which produce a ca. 20-kDa heat-labile metalloprotease toxin (*B. fragilis* toxin, or BFT) have been associated with noninvasive diarrheal disease in animals and young children (21, 28, 29, 32, 34). In addition, recent data suggest that *B. fragilis* isolated from the bloodstream and other extraintestinal sites (e.g., intraabdominal abscesses) may also produce BFT, but correlations with severity or mortality of clinical disease are not yet available (12, 20, 25). BFT stimulates intestinal epithelial cell morphologic changes both in vivo and in vitro (4, 14, 20, 24, 31, 39). Histologic changes observed in vivo after treatment of animal intestinal tissue with BFT include rounding and exfoliation of intestinal epithelial cells as well as submucosal inflammation. These histologic changes are associated with secretion in ileal and colonic ligated intestinal segments in rats, rabbits, and lambs (24). BFT also alters the morphology of immortalized human intestinal epithelial cells in vitro, in particular the cloned cell line HT29/C1 (14, 20, 31, 39, 40). Subconfluent HT29/C1 cells are exquisitely sensitive to BFT, with as little as 0.01 ng/ml (0.5 pM) stimulating morphologic changes that include cell rounding and dissolution of tight clusters after 18 h of incubation (31). These morphologic changes are associated with F-actin redistribution in the cells, with increased F-actin staining at the cell periphery and development of F-actin-containing membrane blebs (4, 14). Although BFT has been shown to cleave monomeric (G) actin in vitro (19), neither quantitative changes in F-actin nor proteolysis is detectable in intact HT29/C1 cells, indicating that BFT does not act by direct proteolysis of cellular actin (30). BFT also stimulates a rapid and persistent increase in HT29/C1 cell volume, an effect apparently linked to the effect of BFT on cellular morphology (14). Although the morphologic effects of BFT appear to be linked to pathophysiologic changes (i.e., secretion in vivo [24] and cell volume changes in vitro [14]), the mechanisms by which BFT may contribute to the pathogenesis of ETBF-associated diarrheal disease remain unclear.

Thus, to develop a model potentially useful for investigations of the mechanisms by which BFT may contribute to diarrheal disease, we evaluated the activity of BFT on monolayers of human intestinal epithelial cells in vitro. For these experiments, we chose T84 cells, which are a well-characterized model of an intestinal chloride-secreting crypt cell (2). Previous experiments in our laboratory have shown that T84 cells are susceptible to the activity of BFT (39). Our results show that BFT alters the function and structure of T84 monolayers in a strikingly polar manner, and counterintuitive to standard concepts of pathogenesis of enteric infections, BFT is more active at the basolateral than the apical membrane of polarized intestinal epithelial cells.

* Corresponding author. Mailing address: Johns Hopkins University School of Medicine, Ross Building, Room 933, 720 Rutland Ave., Baltimore, MD 21205. Phone: (410) 955-9680. Fax: (410) 955-9677. E-mail: csears@welchlink.welch.jhu.edu.

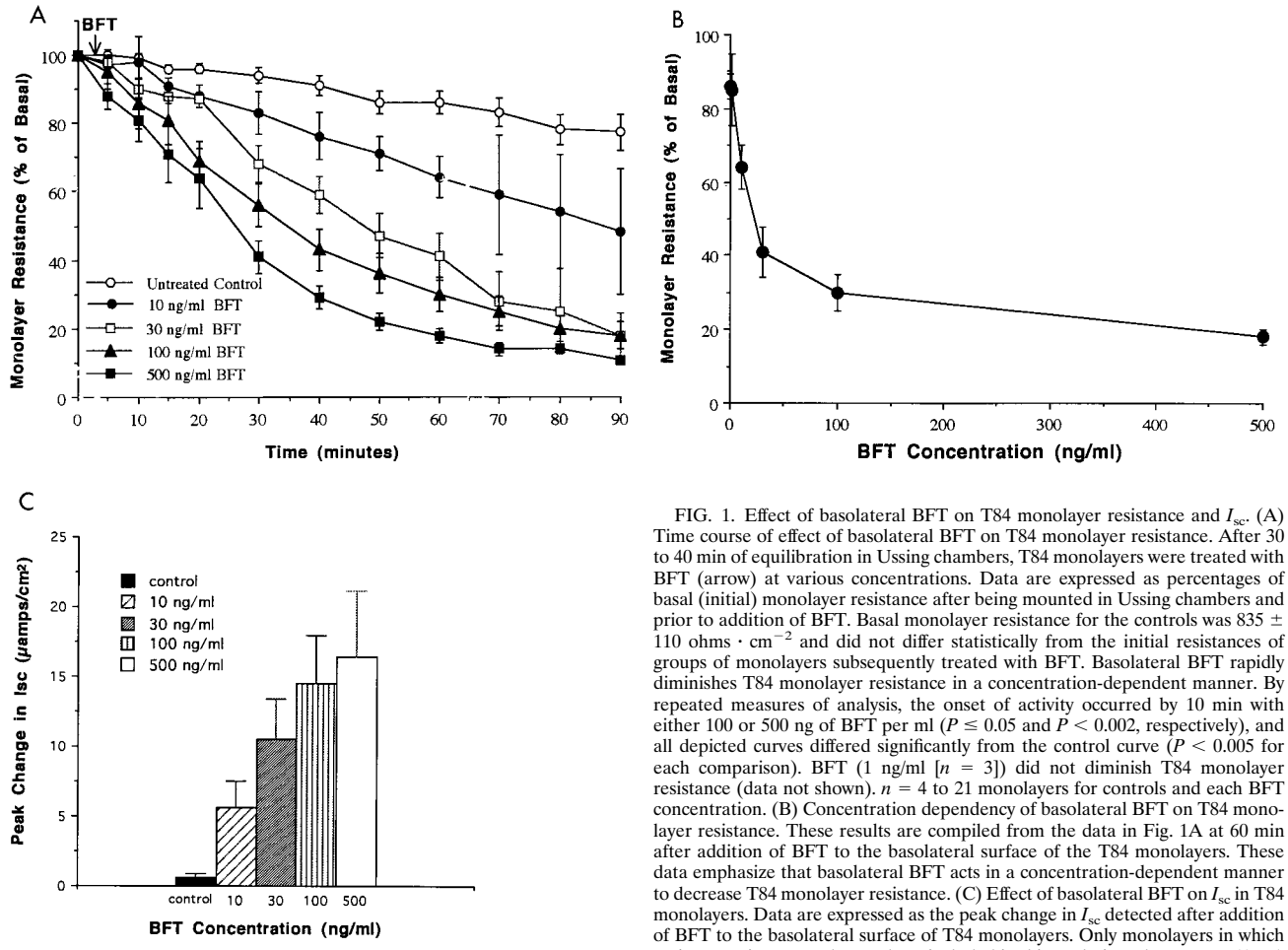

FIG. 1. Effect of basolateral BFT on T84 monolayer resistance and I_{sc}. (A) Time course of effect of basolateral BFT on T84 monolayer resistance. After 30 to 40 min of equilibration in Ussing chambers, T84 monolayers were treated with BFT (arrow) at various concentrations. Data are expressed as percentages of basal (initial) monolayer resistance after being mounted in Ussing chambers and prior to addition of BFT. Basal monolayer resistance for the controls was 835 ± 110 ohms · cm^{-2} and did not differ statistically from the initial resistances of groups of monolayers subsequently treated with BFT. Basolateral BFT rapidly diminishes T84 monolayer resistance in a concentration-dependent manner. By repeated measures of analysis, the onset of activity occurred by 10 min with either 100 or 500 ng of BFT per ml ($P \leq 0.05$ and $P < 0.002$, respectively), and all depicted curves differed significantly from the control curve ($P < 0.005$ for each comparison). BFT (1 ng/ml [$n = 3$]) did not diminish T84 monolayer resistance (data not shown). $n = 4$ to 21 monolayers for controls and each BFT concentration. (B) Concentration dependency of basolateral BFT on T84 monolayer resistance. These results are compiled from the data in Fig. 1A at 60 min after addition of BFT to the basolateral surface of the T84 monolayers. These data emphasize that basolateral BFT acts in a concentration-dependent manner to decrease T84 monolayer resistance. (C) Effect of basolateral BFT on I_{sc} in T84 monolayers. Data are expressed as the peak change in I_{sc} detected after addition of BFT to the basolateral surface of T84 monolayers. Only monolayers in which an increase in I_{sc} was detected are included in this analysis and represent 43, 75, and 83% of monolayers treated with 30 ($n = 14$), 100 ($n = 16$), and 500 ($n = 12$) ng of BFT per ml, respectively. These data indicate that in a subset of monolayers, basolateral BFT (30 ng/ml or more) stimulates a concentration-dependent increase in I_{sc} ($P < 0.001$ for 30, 100, or 500 ng of BFT per ml versus control). Small increases in I_{sc} (3.75 and 7.5 μA/cm^2) were observed in two of four T84 monolayers treated with 10 ng of basolateral BFT per ml. No effect of apical BFT on I_{sc} was detected at any time point (data not shown).

MATERIALS AND METHODS

Cell culture and filter preparation. T84 cells obtained from D. Jefferson (New England Medical Center, Boston, Mass.) were grown in a 1:1 mixture of Dulbecco's modified Eagle's medium and Ham's F-12 medium supplemented with 44 mM sodium bicarbonate, 50 U of penicillin per ml, 50 μg of streptomycin per ml, and 10% fetal bovine serum. Cultures were incubated at 37°C in a humidified atmosphere of 5% CO_2–95% air. Medium was changed three times per week, and cells were used for approximately 11 passages after initial growth from frozen stocks of cells at passage 25. After suspension in 0.25% trypsin–2.65 mM EDTA solution (Gibco, Grand Island, N.Y.), T84 cells were plated on Cylopore polyethylene terephthalate membranes (Falcon Filters; Becton Dickinson and Co., Franklin Lakes, N.J.), tissue culture-treated polycarbonate membranes (Costar-3412 Transwells; Costar, Cambridge, Mass.), or collagen-coated polycarbonate filters as previously described (15, 33). In general, monolayers were studied with Ussing chambers and other assays 11 to 18 days postplating on collagen-coated or Falcon filters. Monolayers were studied 8 to 10 days postplating on Costar filters for immunofluorescence and electron microscopy experiments.

Ussing chamber-voltage clamp transport studies. Transepithelial transport studies were carried out with Ussing chambers (transport aperture, 0.8 cm^2) designed for the study of filter-grown cells (Medical Research Apparatus, Clearwater, Fla.) as previously described (15, 33). Measurements of short circuit current (I_{sc}) were made at 5- to 10-min intervals under voltage-clamped conditions; monolayer resistance was calculated at each time point from the open circuit measurements of potential difference by Ohm's law. Previous data from our laboratory indicated that the fetal calf serum used in T84 cell maintenance inhibited the activity of BFT (20). Thus, for longer time course experiments, T84 monolayers were treated with apical or basolateral BFT in T84 medium with 0.1% bovine serum albumin prior to being mounted in Ussing chambers.

Cell viability studies. Protein synthesis and lactate dehydrogenase (LDH) release assays were used to assess cell viability (14). To measure protein synthesis, T84 cells grown on Falcon filters were treated with 1 μg of basolateral BFT per ml for 2.5 h in the presence of T84 medium containing 1 μCi of [^{3}H]leucine per ml. After incubation with the toxin, the filters were washed, and cellular protein was precipitated with 1 ml of cold 10% trichloroacetic acid for 1 h at 4°C. After aspiration of the trichloroacetic acid, the precipitated proteins were dissolved in 1 ml of 2 N NaOH for 2 h at room temperature. Samples were neutralized with 200 μl of concentrated HCl, and 50 μl of the sample was counted in a scintillation counter.

LDH release was measured after incubation of T84 cells with 1 μg of basolateral BFT per ml for 2.5 h. The apical and basolateral media were collected and analyzed for LDH activity. Total cellular LDH was measured in 0.1% Triton X-100 monolayer extracts (20 min at room temperature). All samples were stored at −20°C until assayed by spectrophotometric assay for LDH as previously described (9). The results shown are percentages of total LDH activity (micromoles per milliliter per minute) released.

F-actin staining. In initial F-actin staining experiments, T84 cells were grown on Costar filters, Falcon filters, or aluminum oxide (Anotec; Nunc, Roskilde, Denmark) membrane filters to determine the best preparation for fluorescence microscopy ($n = 2$). T84 monolayers plated on Costar filters yielded the least background fluorescence. Thus, 8- to 10-day-old monolayers grown on Costar filters were used to investigate the effect of basolateral BFT (500 ng/ml, 2 h) on F-actin structure in T84 monolayers. After the selected incubation time, BFT-treated monolayers or controls were washed with phosphate-buffered saline, fixed with 3.7% formaldehyde for 10 min, and permeabilized with 0.5% Triton X-100 for 5 min. After air drying, the cells were stained with rhodamine-labeled phalloidin (Molecular Probes, Eugene, Oreg.) for 30 min in the dark, washed twice with phosphate-buffered saline and once with double-deionized water, and then examined by confocal microscopy ($n = 6$).

Light and electron microscopy. T84 cells grown on Costar filters for 8 to 10 days were treated with 100 or 500 ng of apical or basolateral BFT per ml for various times. For light microscopy, monolayers were either fixed in 10% buffered formalin, embedded in paraffin, and sectioned at 5 μm prior to staining with hematoxylin and eosin or fixed in 3% glutaraldehyde, embedded in plastic, and sectioned at 1 μm prior to staining with toluidine blue. For transmission electron microscopy (TEM), monolayers were fixed in 3% glutaraldehyde prior to ultrathin sectioning and examination in a Phillips CM12 transmission electron microscope. For scanning electron microscopy (SEM), glutaraldehyde-fixed samples were dehydrated with Peldri (Ted Pella, Inc., Redding, Calif.) and coated with gold-palladium prior to viewing in a Jeol 35C scanning electron microscope.

Purification of BFT. BFT was purified from ETBF VPI 13784 (lamb) or 86-5443-2-2 (piglet) as described by Van Tassell et al. (38). BFT purified from ETBF VPI 13784 was a gift from the laboratory of Tracy Wilkins (Virginia Polytechnic Institute and State University, Blacksburg, Va.). Analytical reverse-phase fast protein liquid chromatography (Pharmacia, Inc., Piscataway, N.J.) was performed with the purified toxin preparation from ETBF 86-5443-2-2 to assess the purity of the sample (41). Approximately 80 μg of BFT was injected onto a PepRPC reverse-phase column equilibrated with water–0.05% trifluoroacetic acid. Protein was eluted with a 0 to 100% gradient of acetonitrile–0.05% TFA over 2 h. Eluted protein was detected by UV A_{226}. 86-5443-2-2 BFT eluted as a single sharp peak at approximately 41% acetonitrile, indicating that the toxin preparation contained a single protein which was ≥95% pure. Purified BFT was maintained at −70°C in a 0.05 M Tris–0.18 M NaCl buffer (pH 7.5) until use.

Neutralization experiments. Polyclonal antisera were produced to BFT purified from ETBF 86-5443-2-2 as previously described (20). For neutralization experiments, heat-inactivated (56°C, 30 min) anti-BFT serum (1/50 dilution) was incubated with 100 ng of BFT per ml for 60 min at room temperature prior to addition to the basolateral membrane of polarized T84 monolayers for 2 h at 37°C. Monolayers were then mounted in Ussing chambers, and electrophysiologic measurements were made as previously described.

Analysis. The data are expressed as means ± standard errors unless specifically stated to be representative experiments. Concentrations causing half-maximal changes were calculated by Lineweaver-Burke transformations of the Michaelis-Menten kinetics for each data set. Student's *t* test was used to determine statistical significance for differences between means. To compare time-dependent and time-of-onset differences, repeated measures of analyses were performed with SAS software.

RESULTS

Effect of apical and basolateral BFT on T84 monolayers. In initial experiments, various concentrations of BFT (100 to 1,000 ng/ml) were added to the apical surface of T84 monolayers (termed "apical BFT") mounted in Ussing chambers. Over the ensuing 2 h, only modest decreases in monolayer resistance (ca., 15 and 25% after treatment with 100 and 1,000 ng of apical BFT per ml, respectively [compared to control monolayers]; $n = 6$ to 8 monolayers per BFT concentration) and no changes in I_{sc} or potential difference were identified (data not shown). With repeated measures of analysis to evaluate the curves, only treatment of T84 monolayers with 1,000 ng of apical BFT per ml significantly decreased monolayer resistance by 2 h ($P < 0.02$ versus control monolayers [data not shown]). In contrast, addition of BFT to the basolateral surface of T84 monolayers stimulated a concentration- and time-dependent decrease in monolayer resistance (Fig. 1A). The activity of basolateral BFT was rapid, occurring by 10 min in response to higher concentrations of BFT ($P \leq 0.05$ and $P < 0.002$ for 100 and 500 ng of BFT per ml, respectively). With repeated measures of analyses to evaluate the curves, T84 monolayers treated with each concentration of BFT depicted were significantly different from control monolayers ($P < 0.005$ for each comparison). T84 monolayers treated with 10 or 30 ng of BFT per ml, but not 100 ng of BFT per ml, differed significantly from monolayers treated with 500 ng of BFT per ml ($P < 0.0005$ for each comparison). The resistances of monolayers treated with 1 ng of basolateral BFT per ml ($n = 3$) were indistinguishable from those of control monolayers (data not shown). Figure 1B illustrates the concentration dependence of the action of BFT assessed 60 min after treatment of the monolayer with basolateral BFT. The BFT concentration resulting in a half-maximal decrease in monolayer resistance was ca. 20 ng/ml (1 nM). The effect of basolateral BFT (100 ng/ml) on T84 monolayer resistance was inhibited ca. 75% by anti-BFT serum, and the effect of BFT on monolayer resistance was reversible over 24 to 48 h when monolayers were treated with lower (25 ng/ml) but not higher (100 ng/ml) concentrations of BFT (data not shown).

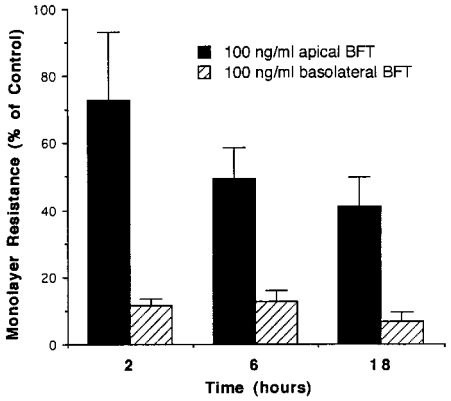

FIG. 2. Comparison of effect of apical and basolateral BFT on T84 monolayer resistance over time. For these experiments, T84 monolayers were treated with apical or basolateral BFT (100 ng/ml) for various times prior to mounting in Ussing chambers. Results are expressed as the percentage of control monolayer resistance measured 60 min after mounting in Ussing chambers. Apical BFT significantly decreases T84 monolayer resistance after 6 or 18 h of treatment ($P \leq 0.007$ versus control for each comparison). $n = 3$ to 6 monolayers for control and apical BFT conditions; $n = 2$ for the basolateral BFT conditions.

In contrast to apical BFT, basolateral BFT also stimulated a concentration-dependent increase in the I_{sc} of T84 monolayers (Fig. 1C). However, BFT-stimulated increases in I_{sc} were not observed in all toxin-treated monolayers. The increase in I_{sc} occurred in 43% of monolayers treated with 30 ng of BFT per ml ($n = 14$), 75% of monolayers treated with 100 ng of BFT per ml ($n = 16$), and 83% of monolayers treated with 500 ng of BFT per ml ($n = 12$). The increases in I_{sc} observed were transient and occurred early after BFT addition to the basolateral surface of the monolayers. Interestingly, the time to the peak I_{sc} decreased as the concentration of BFT was increased. For example, the peak I_{sc} responses to 30, 100, and 500 ng of basolateral BFT per ml occurred at means (± standard error) of 39 ± 3, 23 ± 2, and 14 ± 1 min, respectively ($P < 0.005$ for comparisons of either 30 versus 100 ng/ml or 100 versus 500 ng/ml). It is important to note that BFT-stimulated increases in I_{sc} occurred prior to substantial decreases in monolayer resistance (i.e., before monolayer resistance decreased below 60% of the basal or initial monolayer resistance). The BFT concentration resulting in a half-maximal increase in I_{sc} was also ca. 20 ng/ml (1 nM).

To determine if longer periods of incubation of T84 monolayers with apical BFT would lead to greater changes in monolayer resistance, monolayers were incubated with either 100 or 500 ng of apical BFT per ml for time points of 2 to 18 h prior to being mounted in Ussing chambers for electrophysiologic measurements (Fig. 2). Additional monolayers were treated with basolateral BFT for comparison. These experiments revealed that apical BFT slowly diminishes T84 monolayer resistance, with a maximal reduction of ca. 50% observed 6 h after application of BFT to the apical surface ($P \leq 0.007$ for 6- and 18-h BFT-treated monolayers versus control). No greater effect on T84 monolayer resistance was observed with 500 ng of BFT per ml (data not shown). Consistent with the data in Fig. 1A and B, basolateral BFT (100 ng/ml) rapidly and nearly

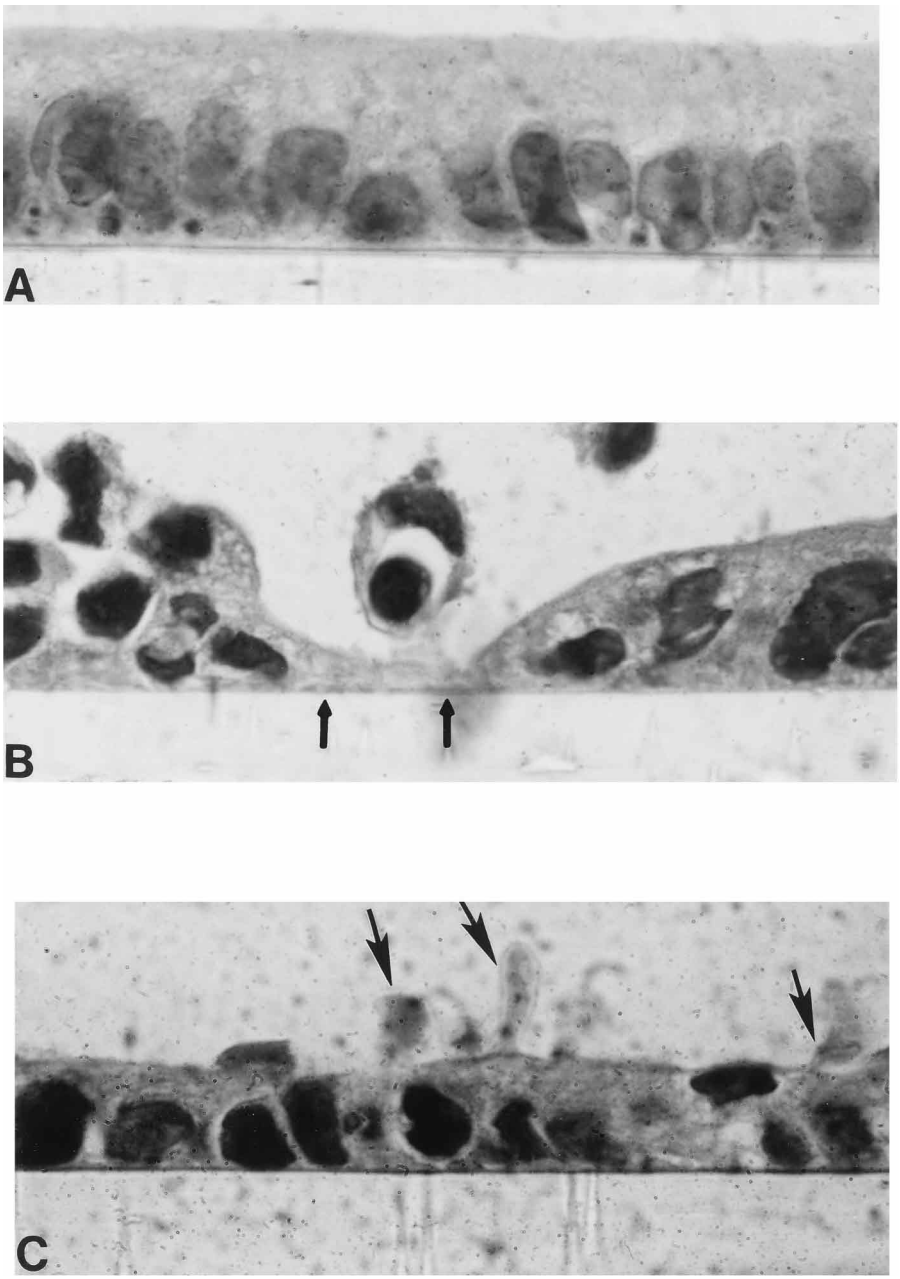

FIG. 3. Effect of apical BFT on the histology of T84 monolayers by light microscopy. After treatment of the monolayers with apical BFT (500 ng/ml) for the indicated time, the monolayers were stained with hemotoxylin and eosin as described in Materials and Methods. (A) Morphology of control T84 monolayers revealing columnar cells with basal nuclei and an intact microvillus membrane. (B) Example of the focal cell loss and morphology changes in the monolayer detected after 18 h of apical BFT treatment. Although BFT does not cause detectable injury to T84 monolayers (see "Effect of BFT on viability of T84 monolayers"), these infrequent detaching cells appear necrotic. Of note, extensions of adjacent epithelial cells were commonly noted to seal the site of any focal cell loss (arrow). (C) Examples of large apical membrane eruptions (arrows) identified in the monolayers after 18 h of apical BFT treatment. Similar, but less dramatic, eruptions of the apical membrane were noted after 6 h of BFT treatment. Magnification, ×1,000.

completely ablated the resistance of T84 monolayers (Fig. 2). No increase in I_{sc} in response to BFT was observed in these experiments.

Effect of BFT on the morphology of T84 Monolayers by light and electron microscopy. Control monolayers revealed columnar epithelial cells with basally located nuclei (Fig. 3A). Beginning 6 h after treatment with apical BFT (100 or 500 ng/ml), focal changes in the morphology of cells in T84 monolayers were identified. These changes included small groups of rounded cells, the loss of occasional cells from the monolayer, and eruptions of the apical membrane of the cells. Cellular morphologic changes after BFT were similar, but more pronounced, after 18 h of apical BFT treatment (Fig. 3B and C). An interesting observation was that epithelial extensions commonly covered the filter at sites at which an epithelial cell was exfoliating. In contrast, treatment of monolayers with basolateral BFT led to morphologic changes in nearly every cell in the monolayer after only 90 min of incubation with toxin (Fig. 4).

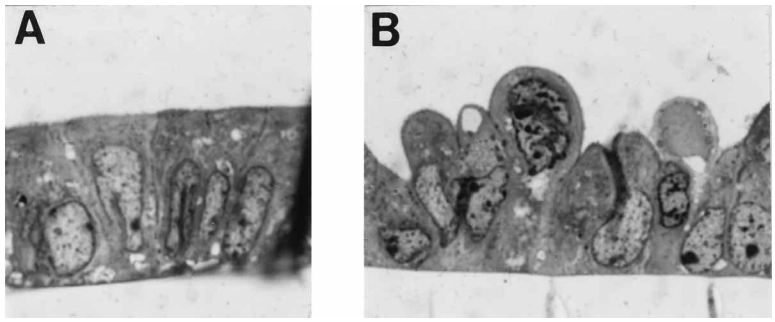

FIG. 4. Effect of basolateral BFT on the histology of T84 monolayers by light microscopy. T84 monolayers were treated with basolateral BFT (100 ng/ml) for 90 min prior to fixation and staining with toluidine blue as described in Materials and Methods. In contrast to the focal morphologic changes noted after apical BFT treatment (Fig. 3B and C), morphologic changes are observed in nearly every cell in the monolayer. Notable morphologic changes included rounding of the apical membrane, loss of cell height, and apical drift of the nuclei. Magnification, ×1,000.

The morphologic changes after basolateral BFT were considerably more dramatic, with cell rounding, ballooning of the apical membranes of the cells, and apical drift of the nuclei. Similar to the observations with apical BFT, adjacent epithelial cells were nearly always observed to be sealing the site of an exuding epithelial cell.

Because of the dramatic morphologic changes observed in response to basolateral BFT, the effect of basolateral BFT on T84 cell morphology was further examined by TEM and SEM. Compared to control monolayers (Fig. 5A), T84 monolayers treated with 100 ng of basolateral BFT per ml for 2 h revealed apparent cell swelling, a cuboidal morphology, and a striking loss of microvilli by TEM (Fig. 5B). In addition, hyperconvolution and modest chromatin margination were noted in the nuclei of BFT-treated cells. Comparison of control (Fig. 5C) and BFT-treated intercellular junctions revealed that the zonula occludens and zonula adherens appeared denser and less elongated after treatment of the monolayers with 100 ng of basolateral BFT per ml (Fig. 5D), whereas complete disruption of the zonula occludens and zonula adherens of some, but not all, junctional complexes was observed after treatment of the monolayers with 500 ng of basolateral BFT per ml (Fig. 5E). In contrast, the desmosomes (which anchor intermediate filaments composed of keratin to the plasma membrane) of the BFT-treated monolayers appeared intact. SEM of monolayers treated with 500 ng of basolateral BFT per ml (Fig. 5G) revealed a complete loss of the interdigitated appearance of the apical membrane of the cells, indicating loss of the microvilli when compared to control monolayers (Fig. 5F).

Effect of BFT on the F-actin structure of T84 monolayers. To assess the effect of BFT on the F-actin structure of T84 monolayers at times of maximal decreases in monolayer resistance, T84 monolayers were treated with 500 ng of basolateral BFT per ml for 2 h, stained with rhodamine-labelled phalloidin, which binds specifically to F-actin, and examined by confocal microscopy. Control monolayers revealed a honeycomb pattern of fluorescence at the periphery of the cells consistent with the F-actin-enriched tight junctions as well as punctate surface staining consistent with the F-actin bundles present in the apical microvilli (Fig. 6A). At the basal pole of the control monolayers, F-actin microfilaments were detected at sites of focal contacts linking actin microfilaments to the extracellular matrix or filter (Fig. 6C). In contrast, after basolateral BFT treatment, the monolayers revealed diminished F-actin staining in the apical microvilli and at the level of the tight junctions (Fig. 6B). In some regions, the F-actin staining appeared more floccular or plaquelike in the tight junctional ring at the apical pole of the monolayers. At the basal pole of the monolayers, enhanced F-actin staining with thickening of the microfilament bundles was detected at the sites of focal contacts (Fig. 6D). In the representative F-actin staining experiment shown here, parallel monolayers were treated with basolateral BFT and examined in Ussing chambers. The control monolayers in this experiment had resistances of 2,400 and 1,829 ohms · cm^{-2}, whereas monolayers treated with 500 ng of basolateral BFT per ml developed marked reductions in resistance after 2 h (304 and 200 ohms · cm^{-2}).

Effect of BFT on viability of T84 monolayers. Because a reduction in the resistance of T84 monolayers could indicate that BFT was fatally injuring the cells, T84 monolayers treated with 1 μg of basolateral BFT per ml for 2.5 h (i.e., a concentration and time point correlating with maximal decreases in T84 monolayer resistance) were assessed by LDH release and protein synthesis assays. These experiments revealed that treatment of monolayers with BFT (1 μg of basolateral BFT per ml for 2.5 h) did not result in release of LDH (14.4% ± 5.8% of total cellular LDH for BFT-treated monolayers versus 9.2% ± 3.5% for controls; $n = 6$ paired measurements, with P not significant versus controls) into either the apical or basolateral medium bathing the cells. However, BFT treatment of the monolayers did stimulate a significant increase in [^{3}H]leucine uptake by the cells (33,311 ± 2,744 cpm/monolayer) compared to that by the controls (27,086 ± 2,096 cpm/monolayer) ($n = 4$ paired measurements, with $P = 0.007$ versus controls).

DISCUSSION

The key observation from these experiments is that the effect of BFT on monolayers of human intestinal epithelial cells in vitro is polar. Namely, the biological activity of BFT is greater when BFT is applied to the basolateral surface of the monolayers and results in functional and structural changes in the apical membrane of the monolayers. The polar activity of BFT was observed with all parameters measured, including monolayer resistance, increases in I_{sc} (indicative of chloride secretion), morphology of the cells, and F-actin cellular structure after BFT treatment. Similarly, polar activity of BFT has been observed on HT29/C1, uncloned HT29, and MDCK (Madin-Darby canine kidney) cell monolayers (6b, 23), and human colon examined in vitro (27). Although this site of action is counterintuitive for an enteric pathogen or toxin, both *Shigella* spp. (7) and *Listeria monocytogenes* (18) are known to invade intestinal epithelial cells via their basolateral membranes (albeit after initial entry through intestinal M cells). In contrast, ETBF organisms have not been observed to be invasive in

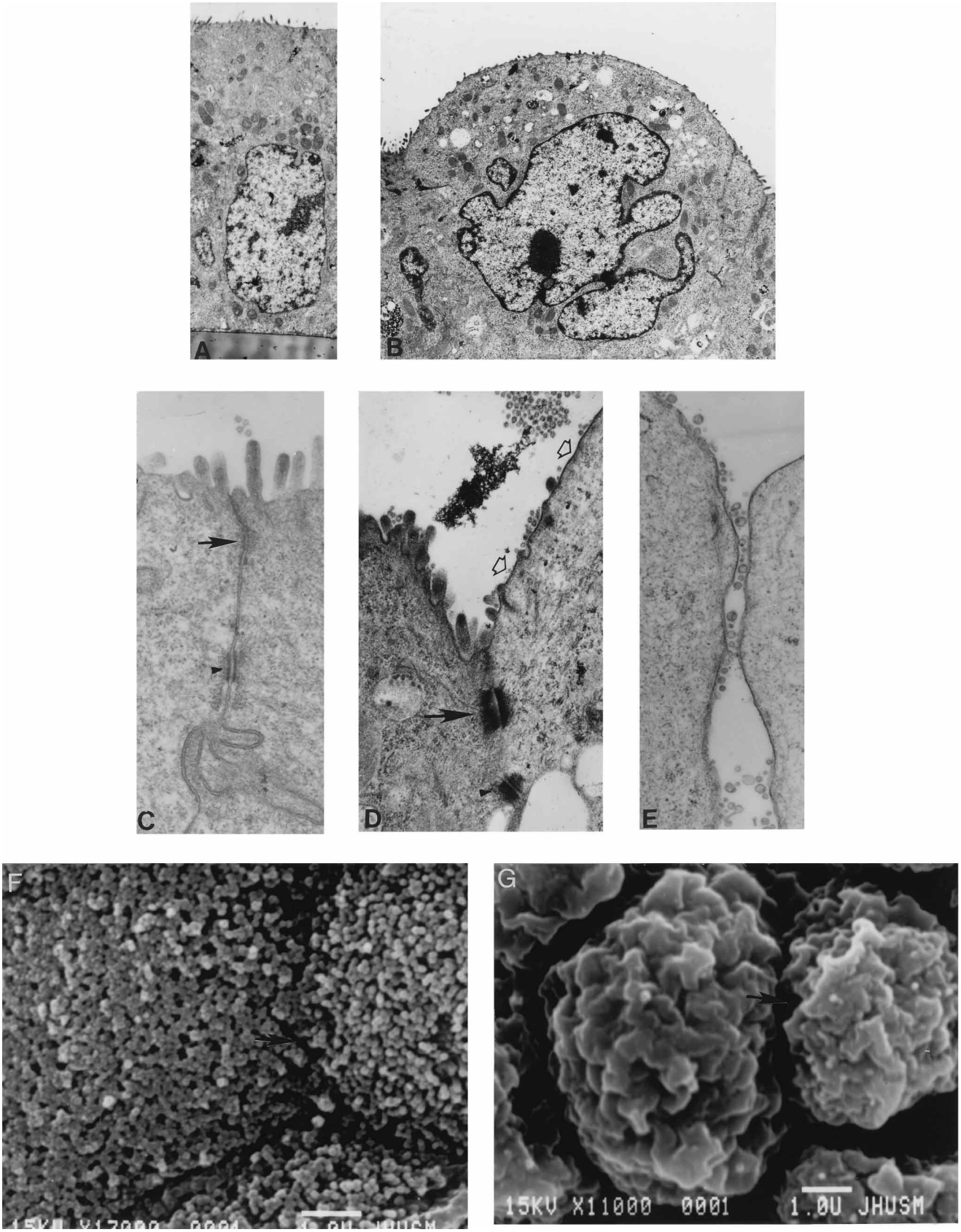
A
B
C
D
E
F
G
15KV X11000 0001 1.0U JHUSM

animal studies (22). Distal signalling to the apical membrane of intestinal epithelial cells resulting in chloride secretion has also been observed in response to carbachol, an acetylcholine analog which acts at the basolateral membrane to stimulate phospholipase Cγ, leading to an increase in intracellular calcium and activation of protein kinase C (13).

Particularly intriguing is our observation that the structure of the apical pole of T84 cells is remarkably altered with nearly complete loss of the microvilli after basolateral BFT treatment. Consistent with this morphologic change, F-actin staining was diminished at the apical pole of the cells, most likely due to depolymerization of the actin bundles present in the microvilli, with additional changes occurring in the apical actin belt, which is tethered to the zonula occludens and zonula adherens in polarized intestinal epithelial cells (1, 5). Despite the evidence of diminished F-actin detectable in the structures at the apical membrane, increased staining of microfilaments was observed at the basal pole of the cells, suggesting that F-actin is redistributed in the cells after BFT treatment but that total F-actin content may not be altered. In support of this concept, BFT alters the distribution but not the amount of F-actin detectable in HT29/C1 cells when quantitated with 7-nitrobenz-2-oxa-1,3-diazole–phallicidin (30). Furthermore, no evidence to date suggests BFT can enter cells (23, 31), and proteolysis of actin is not identifiable in HT29/C1 cells, suggesting that although BFT can cleave G actin in vitro (19), direct cleavage of actin by BFT in HT29/C1 cells does not appear to occur (30). Polar changes in F-actin staining have also been observed in Caco-2 cells (another human intestinal epithelial cell line) after overexpression of villin antisense RNA (3). In these cells, diminished villin expression leads to an increase in F-actin microfilaments at the basal pole of Caco-2 cells with associated loss of apical F-actin staining. The appearance of the apical membrane of T84 monolayers after basolateral BFT treatment suggests loss of F-actin bundling by villin and/or fimbrin after BFT treatment, and we hypothesize that this may precipitate redistribution of F-actin to the basal pole of the monolayers. Interestingly, treatment of T84 monolayers with either cyclic AMP-dependent agonists (35) or the heat-stable enterotoxin (STa) of *Escherichia coli* (16) also stimulates increased F-actin microfilament staining at the basal pole of the monolayers.

The experiments reported here demonstrate an excellent correlation between the structure and function of T84 monolayers after BFT treatment. Namely, treatment of T84 monolayers with apical BFT slowly resulted in focal morphologic changes, with evidence of epithelial barrier repair at sites of exuding cells, and hence only a 50% decrease in monolayer resistance was observed 6 h after incubation with BFT. In contrast, treatment of the monolayers with basolateral BFT rapidly altered the morphology of nearly every cell in the monolayer, a result consistent with its activity to rapidly and nearly completely ablate T84 monolayer resistance. Similar reductions in the resistance are observed after treatment of HT29 cell monolayers or polarized monolayers of nonintestinal cells (MDCK, rat lung type II cells) with BFT (6a, 23, 40). The loss of T84 monolayer resistance in response to treatment with basolateral BFT was associated with, in some instances, gross disruption of the zonula occludens (or tight junction) and zonula adherens. The latter observation, combined with our observation of only a transient increase in I_{sc} after BFT treatment, indicates that BFT reduces monolayer resistance primarily by altering paracellular permeability (1) and thus can be added to the growing list of enteric pathogens (e.g., enteropathogenic *E. coli* [26, 36] and *Salmonella typhimurium* [17]) and toxins (e.g., *Clostridium difficile* toxins A and B [8, 9] and zonula occludens toxin [6]) which alter intestinal permeability. Our data are also consistent with recent data reported by Obiso et al. (23) showing an increase in [^{3}H]mannitol flux in BFT-treated epithelial monolayers, indicating a change in tight junctional function. The striking loss of T84 cell height noted after basolateral BFT treatment (Fig. 5B) may be due to a change in cell volume (14) and/or the F-actin changes stimulated by BFT (Fig. 6). The morphologic observations in T84 monolayers reported here are very similar to previous observations of the ultrastructural appearance of lamb intestine after infection with ETBF organisms (32a, 37). Consistent with prior observations in HT29, MDCK, and HT29/C1 cells (14, 23), these dramatic morphologic changes occur without fatal injury to T84 cells, and in fact, recovery of monolayer resistance occurs after treatment with lower concentrations of BFT (this study and reference 23).

We also detected chloride secretion in response to treatment of some T84 monolayers with basolateral BFT. This effect of BFT was early, transient, and dose dependent but intermittent, prohibiting more-detailed studies. We have similarly observed that BFT can stimulate an increase in I_{sc} in HT29/C1 monolayers, but only if the initial PD of the monolayer was $\geq$1 mV (6a). Although a mechanistic explanation for these observations is not yet available, we hypothesize that the I_{sc} response to BFT may require potentiation by an as yet unidentified mediator. The early and transient nature of the I_{sc} response observed suggests that the initial changes in the apical membrane (which ultimately result in a dramatic loss of microvilli) may alter the regulation of one or more apical membrane ion transporters.

The results reported here provide an important contrast to prior results in T84 monolayers treated with *C. difficile* toxins A and B (8, 9). Both toxins A and B stimulate a marked reduction in T84 monolayer resistance in a time- and concentration-dependent manner. However, both toxins act more slowly than BFT to alter the function of T84 monolayers and were equally effective at the apical and basolateral membranes of the monolayers (8, 9). Furthermore, despite the ability of toxins A and B to nearly ablate monolayer resistance, ultrastructural changes in T84 cells were not observed (i.e., tight junctions and microvillus membranes appeared similar to those in control cells). However, both toxins altered the F-actin structure of

FIG. 5. Effect of basolateral BFT on the morphology of T84 monolayers by electron microscopy. (A and B) Appearance of control (A) and BFT-treated (B [100 ng/ml, 2 h]) T84 monolayers by TEM. Compared to a control cell, T84 cells treated with basolateral BFT appear swollen and cuboidal and exhibit nearly complete loss of their interdigitated microvillus membranes leading to ballooning of the apical membrane. Nuclei of the cells reveal hyperconvolution and modest chromatin margination and appear to drift from the basal pole towards the apical pole of the cells. Magnification, ×3,000. (C to E) Appearance of the zonula occludens (ZO) (arrow) and zonula adherens (ZA) (arrowhead) in control (C) and BFT-treated (100 [D] versus 500 [E] ng/ml) monolayers. After treatment with 100 ng of basolateral BFT per ml, the ZO and ZA appear denser and less elongated. Effacement of the apical membrane of one cell has occurred (open arrow). In contrast, after treatment with 500 ng of basolateral BFT per ml, some, but not all, ZO and ZA in the monolayers were found to be completely open. In adjoining cells lacking the ZO and ZA, complete effacement of the adjacent microvillus membranes of the affected cells was observed. Magnification, ×12,750. (F) Appearance by SEM of the apical membrane of control T84 monolayers. The intercellular junction is marked with an arrow. (G) Appearance of the apical membrane after treatment of the monolayers with 500 ng of basolateral BFT per ml for 2 h. In contrast to the tightly organized microvilli of control monolayers, the apical membranes of the cells after basolateral BFT no longer have identifiable microvilli, and separation of the intercellular junctions after BFT treatment is observed (arrow). Magnifications: ×9750, control; ×8,250, BFT.

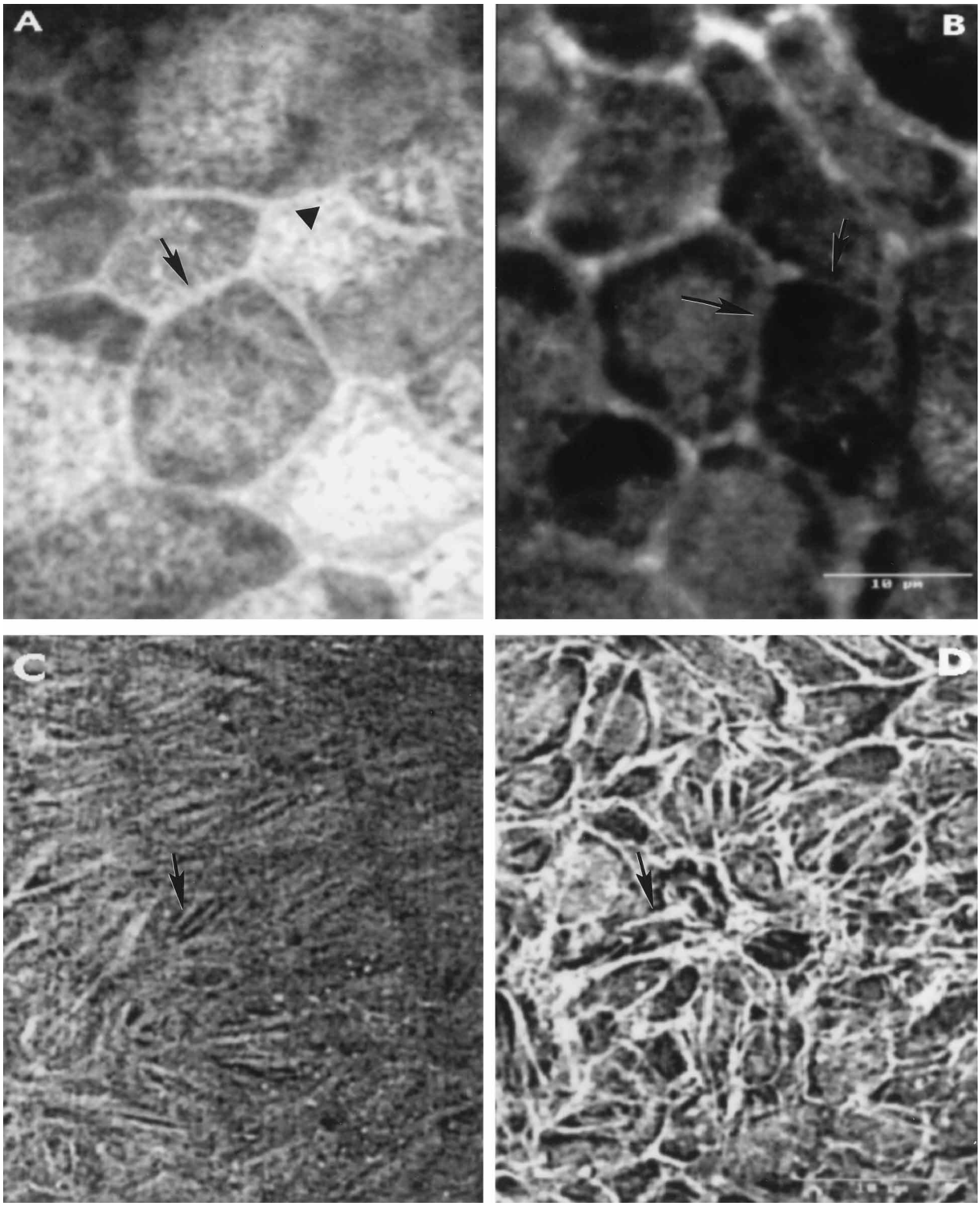

FIG. 6. Appearance of F-actin staining by confocal microscopy after treatment of T84 monolayers with basolateral BFT. For these experiments, T84 monolayers were treated with 500 ng of basolateral BFT per ml for 2 h prior to fixation, permeabilization, and staining with rhodamine-phalloidin as described in Materials and Methods. (A and B) Appearance of F-actin staining at the apical pole of the monolayer. In the control monolayer (A), an apical ring of actin is identified (arrow) and punctate surface staining (arrowhead) is observed, consistent with staining of the F-actin bundles of the microvilli at this cell surface. In contrast, F-actin staining at the periphery of the cells (arrow) and in the microvilli is diminished after basolateral BFT treatment (B). (C and D) Appearance of F-actin staining at the basolateral pole of the monolayer. In the control monolayer (C), F-actin staining at sites of focal contacts is identified (arrow). In contrast, after BFT treatment (D), F-actin staining at these focal contacts is increased with thickening of the F-actin microfilaments (arrow).

T84 cells, with toxin A appearing to nearly completely depolymerize F-actin and with toxin B resulting in the formation of F-actin-containing plaques, results most likely due to the ability of both toxins to monoglucosylate the small GTP-binding protein rho, which regulates F-actin structure in cells (10, 11). Additional studies examining the action of these toxins on human colon in vitro have revealed that toxins A and B act only at the apical membrane of this tissue and that only morphologic changes in surface colonocytes are observed (27). In contrast, BFT exhibits greater biological activity on human colon in vitro after application to the basolateral (serosal) surface of the tissues and results in rounding of both surface and crypt colonocytes after basolateral BFT but only surface changes after apical BFT (27). Finally, BFT stimulates an increase in HT29/C1 cell volume, whereas treatment with *C. difficile* toxin A decreases HT29/C1 cell volume (14). Together, these observations emphasize that the mechanisms by which these toxins (A and B versus BFT) alter intestinal epithelial function are different.

In conclusion, we believe our data suggest a potential model by which BFT may act to alter intestinal epithelial structure and function, leading to the development of diarrheal disease. ETBF organisms may release BFT in the intestinal lumen, which causes focal histologic changes and initiates a modest increase in the permeability of the intestine. This increase in permeability may facilitate delivery of BFT to the basolateral membranes of the intestinal epithelial cells, where BFT acts rapidly to augment the loss of barrier function of the epithelium and to stimulate chloride secretion. Together, these pathophysiologic changes, decreased barrier function (or altered paracellular transport), and chloride secretion (or altered transcellular transport) would serve to stimulate intestinal secretion, resulting in the clinical outcome of diarrheal disease. In support of this model, preliminary studies in our laboratory indicate that traces of BFT can be detected in the medium bathing the basolateral membranes of T84 monolayers beginning 6 h after treatment of the monolayers with apical BFT (29a). Further studies will be required to substantiate this model and to investigate the functional consequences of the dramatic changes in the apical intestinal membrane observed after exposure to BFT.

ACKNOWLEDGMENTS

This work was supported by NIH grant DK 45496 (to C.L.S.).

We thank Dwight Derr for expert tissue culture preparations; Farifteh Firoozmand, Shaoguang Wu, and Irene Eromar for technical assistance; Michael Delannoy for assistance with confocal microscopy; and Tracy D. Wilkins (Virginia Polytechnical Institute and State University, Blacksburg, Va.) for gifts of purified BFT (supported by NIH grant AI 322940 to T.D.W.).

REFERENCES

1. **Anderson, J. M., and C. M. Van Itallie.** 1995. Tight junctions and the molecular basis for regulation of paracellular permeability. Am. J. Physiol. **269:**G467–G475.
2. **Barrett, K. E.** 1993. Positive and negative regulation of chloride secretion in T84 cells. Am. J. Physiol. **265:**C859–C868.
3. **Costa de Beauregard, M., E. Pringault, S. Robine, and D. Louvard.** 1995. Suppression of villin expression by antisense RNA impairs brush border assembly in polarized epithelial intestinal cells. EMBO J. **14:**409–421.
4. **Donelli, G., A. Fabbri, and C. Fiorentini.** 1996. *Bacteroides fragilis* enterotoxin induces cytoskeletal changes and surface blebbing in HT-29 cells. Infect. Immun. **64:**113–119.
5. **Drubin, D. G., and W. J. Nelson.** 1996. Origins of cell polarity. Cell **84:**335–344.
6. **Fasano, A., C. Fiorentini, G. Donelli, S. Uzzau, J. B. Kaper, K. Margaretten, X. Ding, S. Guandalini, L. Comstock, and S. E. Goldblum.** 1995. Zonula occludens toxin (Zot) modulates tight junctions through protein kinase C-dependent actin reorganization in vitro. J. Clin. Invest. **96:**710–720.

6a. **Firoozmand, F., and C. Sears.** Unpublished observations.
6b. **Firoozmand, F., S. Wu, and C. Sears.** Unpublished observations.

7. **Goldberg, M. B., and P. J. Sansonetti.** 1993. *Shigella* subversion of the cellular cytoskeleton: a strategy for epithelial colonization. Infect. Immun. **61:**4941–4946.
8. **Hecht, G., A. Koutsouris, C. Pothoulakis, J. T. LaMont, and J. L. Madara.** 1992. *Clostridium difficile* toxin B disrupts the barrier function of T_{84} monolayers. Gastroenterology **102:**416–423.
9. **Hecht, G., C. Pothoulakis, J. T. LaMont, and J. L. Madara.** 1988. *Clostridium difficile* toxin A perturbs cytoskeletal structure and tight junction permeability of the cultured human intestinal epithelial monolayers. J. Clin. Invest. **82:**1516–1524.
10. **Just, I., J. Selzer, M. Wilm, C. von Eichel-Streiber, M. Mann, and K. Aktories.** 1995. Glucosylation of Rho proteins by *Clostridium difficile* toxin B. Nature **375:**500–503.
11. **Just, I., M. Wilm, J. Selzer, G. Rex, C. von Eichel-Streiber, M. Mann, and K. Aktories.** 1995. The enterotoxin from *Clostridium difficile* (ToxA) monoglucosylates the Rho proteins. J. Biol. Chem. **270:**13932–13936.
12. **Kato, N., A. Karuniawati, R. Jotwani, H. Kato, K. Watanabe, and K. Ueno.** 1995. Isolation of enterotoxigenic *Bacteroides fragilis* from extraintestinal sites by cell culture assay. Clin. Infect. Dis. **20**(Suppl. 2)**:**S141.
13. **Khurana, S., S. Kreydiyyeh, W. A. Hoogerwerf, S. G. Rhee, M. Donowitz, and M. E. Cohen.** 1996. Asymmetric signal transduction in polarized ileal Na^+ absorbing cells: carbachol activates brush border but not basolateral membrane PI-PLC and translocates PLC-gamma$_1$ only to the brush border. Biochem. J. **313:**509–518.
14. **Koshy, S. S., M. H. Montrose, and C. L. Sears.** 1996. Human intestinal epithelial cells swell and demonstrate actin rearrangement in response to the metalloprotease toxin of *Bacteroides fragilis*. Infect. Immun. **64:**5022–5028.
15. **Levine, S. A., M. Donowitz, A. J. M. Watson, G. W. G. Sharp, J. K. Crane, and C. S. Weikel.** 1991. Characterization of the synergistic interaction of *Escherichia coli* heat-stable toxin and carbachol. Am. J. Physiol. **261:**G592–G601.
16. **Matthews, J. B., C. S. Awtrey, R. Thompson, T. Hung, K. J. Tally, and J. L. Madara.** 1993. Na^+-K^+-$2Cl^-$ cotransport and Cl^- secretion evoked by heat-stable enterotoxin is microfilament dependent in T84 cells. Am. J. Physiol. **265:**G370–G378.
17. **McCormick, B. A., S. P. Colgan, C. Delp-Archer, S. I. Miller, and J. L. Madara.** 1993. *Salmonella typhimurium* attachment to human intestinal epithelial monolayers: transcellular signalling to subepithelial neutrophils. J. Cell Biol. **123:**895–907.
18. **Mengaud, J., H. Ohayon, P. Gounon, R. Mege, and P. Cossart.** 1996. E-cadherin is the receptor for internalin, a surface protein required for entry of *L. monocytogenes* into epithelial cells. Cell **84:**923–932.
19. **Moncrief, J. S., R. Obiso, Jr., L. A. Barroso, J. J. Kling, R. L. Wright, R. L. Van Tassell, D. M. Lyerly, and T. D. Wilkins.** 1995. The enterotoxin of *Bacteroides fragilis* is a metalloprotease. Infect. Immun. **63:**175–181.
20. **Mundy, L. M., and C. L. Sears.** 1996. Detection of toxin production by *Bacteroides fragilis*: assay development and screening of extraintestinal clinical isolates. Clin. Infect. Dis. **23:**269–276.
21. **Myers, L. L., B. D. Firehammer, D. S. Shoop, and M. M. Border.** 1984. *Bacteroides fragilis*: a possible cause of acute diarrheal disease in newborn lambs. Infect. Immun. **44:**241–244.
22. **Myers, L. L., and C. S. Weikel.** 1992. Enterotoxin as a virulence factor in *Bacteroides fragilis* - associated diarrhoeal disease, p. 90–100. *In* B. I. Duerden, J. S. Brazier, S. V. Seddon, and W. G. Wade (ed.), Medical and environmental aspects of anaerobes. Wrightson Biomedical Publishing, Ltd., Petersfield, United Kingdom.
23. **Obiso, R. J., Jr., A. O. Azghani, and T. D. Wilkins.** 1997. The *Bacteroides fragilis* toxin fragilysin disrupts the paracellular barrier of epithelial cells. Infect. Immun. **65:**1431–1439.
24. **Obiso, R. J., Jr., D. M. Lyerly, R. L. Van Tassell, and T. D. Wilkins.** 1995. Proteolytic activity of the *Bacteroides fragilis* enterotoxin causes fluid secretion and intestinal damage in vivo. Infect. Immun. **63:**3820–3826.
25. **Pantosti, A., M. Cerquetti, R. Colangeli, and F. D'Ambrosio.** 1994. Detection of intestinal and extra-intestinal strains of enterotoxigenic *Bacteroides fragilis* by the HT-29 cytotoxicity assay. J. Med. Microbiol. **41:**191–196.
26. **Philpott, D. J., D. M. McKay, P. M. Sherman, and M. H. Perdue.** 1996. Infection of T84 cells with enteropathogenic *Escherichia coli* alters barrier and transport functions. Am. J. Physiol. **270:**G634–G645.
27. **Riegler, M., M. Lotz, C. L. Sears, C. Pothoulakis, I. Castagliuolo, R. Sedivy, T. Sogukoglu, E. Cosentini, G. Bischof, W. Feil, B. Teleky, G. Hamilton, J. T. LaMont, and E. Wenzl.** Differential effects of *Bacteroides fragilis* toxin (BFT)-2 and *Clostridium difficile* toxins A and B on human colonic mucosa *in vitro*. Submitted for publication.
28. **Sack, R. B., M. J. Albert, K. Alam, P. K. B. Neogi, and M. S. Akbar.** 1994. Isolation of enterotoxigenic *Bacteroides fragilis* from Bangladeshi children with diarrhea: a controlled study. J. Clin. Microbiol. **32:**960–963.
29. **Sack, R. B., L. L. Myers, J. Almeido-Hill, D. S. Shoop, W. C. Bradbury, R. Reid, and M. Santosham.** 1992. Enterotoxigenic *Bacteroides fragilis*: epidemiologic studies of its role as a human diarrhoeal pathogen. J. Diarrhoeal Dis. Res. **10:**4–9.

29a. **Saidi, R., and C. Sears.** Unpublished observations.
30. **Saidi, R. F., K. Jaeger, M. H. Montrose, S. Wu, and C. L. Sears.** 1997. *Bacteroides fragilis* toxin alters the actin cytoskeleton of HT29/C1 cells in vivo qualitatively but not quantitatively. Cell Motil. Cytoskeleton **37:**159–165.
31. **Saidi, R. F., and C. L. Sears.** 1996. *Bacteroides fragilis* toxin rapidly intoxicates human intestinal epithelial cells ($HT29/C_1$) in vitro. Infect. Immun. **64:**5029–5034.
32. **San Joaquin, V. H., J. C. Griffis, C. Lee, and C. L. Sears.** 1995. Association of *Bacteroides fragilis* with childhood diarrhea. Scand. J. Infect. Dis. **27:**211–215.
32a. **Sears, C., and L. Myers.** Unpublished observations.
33. **Sears, C. L., F. Firoozmand, A. Mellander, F. G. Chambers, I. Eromar, A. G. M. Bot, B. Scholte, H. R. de Jonge, and M. Donowitz.** 1995. Genistein and tyrphostin 47 stimulate cystic fibrosis transmembrane conductance regulator-mediated chloride secretion in human intestinal epithelial cell (T84) monolayers. Am. J. Physiol. **269:**G874–G882.
34. **Sears, C. L., L. L. Myers, A. Lazenby, and R. L. Van Tassell.** 1995. Enterotoxigenic *Bacteroides fragilis*. Clin. Infect. Dis. **20**(Suppl. 2)**:**S142–S148.
35. **Shapiro, M., J. Matthews, G. Hecht, C. Delp, and J. L. Madara.** 1991. Stabilization of F-actin prevents cAMP-elicited Cl^- secretion in T84 cells. J. Clin. Invest. **87:**1903–1909.
36. **Spitz, J., R. Yuhan, A. Koutsouris, C. Blatt, J. Alverdy, and G. Hecht.** 1995. Enteropathogenic *Escherichia coli* adherence to intestinal epithelial monolayers diminishes barrier function. Am. J. Physiol. **268:**G374–G379.
37. **Tse, C., S. A. Levine, C. C. H. Yun, S. R. Brant, S. Nath, J. Pouyssegur, and M. Donowitz.** 1994. Molecular properties, kinetics and regulation of mammalian Na^+/H^+ exchangers. Cell. Physiol. Biochem. **4:**282–300.
38. **Van Tassell, R. L., D. M. Lyerly, and T. D. Wilkins.** 1992. Purification and characterization of an enterotoxin from *Bacteroides fragilis*. Infect. Immun. **60:**1343–1350.
39. **Weikel, C. S., F. D. Grieco, J. Reuben, L. L. Myers, and R. B. Sack.** 1992. Human colonic epithelial cells, $HT29/C_1$, treated with crude *Bacteroides fragilis* enterotoxin dramatically alter their morphology. Infect. Immun. **60:** 321–327.
40. **Wells, C. L., E. M. A. Van De Westerlo, R. P. Jechorek, B. A. Feltis, T. D. Wilkins, and S. L. Erlandsen.** 1996. *Bacteroides fragilis* enterotoxin modulates epithelial permeability and bacterial internalization by HT-29 enterocytes. Gastroenterology **110:**1429–1437.
41. **Wu, S., L. A. Dreyfus, A. O. Tzianabos, and C. L. Sears.** Diversity of the metalloprotease toxin produced by enterotoxigenic *Bacteroides fragilis*. Submitted for publication.

Editor: P. E. Orndorff